SURFACE PARAMETERS EVALUATED FROM SATELLITE REMOTE SENSING IMAGES FOR POLLUTANT ATMOSPHERIC DISPERSION MODELLING

Sergio Teggi[1], Maria Paola Bogliolo[2], Grazia Ghermandi[1], Sara Fabbi[1], Marina Funaro[2] and Claudio Gariazzo[2]

[1]University of Modena and Reggio Emilia, Modena, Italy
[2]ISPESL, Monteporzio Catone (Rome), Italy

Abstract: This contribute deals with the use of surface parameters extracted from satellite remote sensing images for the setup of the input dataset required by pollutants atmospheric dispersion models (PATM). These models need 2D distributions (grids) of many surface parameters to model turbulence parameters, as roughness length, albedo, leaf area index and Bowen ratio. Very often these parameters are set using predefined tables defined as a function of land cover (LC). Usually, this last information is extracted from public datasets, such as, for European countries, the CORINE Land Cover (CLC). Some of these parameters can be computed directly from remote sensing. Moreover, land cover classification evaluated from remote sensing can be used to update existing LC datasets. In this work ASTER images have been used to evaluate, using a supervised classification method, the LC map of the area. This LC is used to update the CLC. Moreover, albedo was directly calculated from the image. The importance of information extracted from remote sensing is evaluated using the SPRAY lagrangian PATM. SPRAY has been used to simulate the dispersion of an inert generic pollutant emitted from two virtual sources on a 30 km x 40 km domain in a study area located at Venice (Northern Italy), where a big industrial site is found (Porto Marghera). Real (measured) meteorological data have been used.

Key words: *Remote sensing, lagrangian dipersion model, classification, CORINE land cover, albedo.*

1. INTRODUCTION

The meteorological pre-processors of several pollutant atmospheric dispersion models use land surface properties to model the local mesoscale circulation induced by land surface forcing. Usually they rely on a set of surface biophysical parameters (albedo, roughness length, soil moisture, thermal inertia, etc.) assigned by means of a parameterization scheme to different categories of surface Land Use/Land Cover (LULC). As a consequence, the accuracy of both LULC maps and parameterization schemes is important to obtain accurate simulations. One source of errors concerning LULC maps is the lack of updating, that reduces the representativeness of the actual cover conditions (in particular concerning urbanization that strongly changes the biophysical properties of the surface); the other problem found with LULC maps is the poor link between some LULC categories and a specific-unique value of the surface parameters of interest, due to the fact that usually those maps were produced for different goals. As an example, in a cultivated land, different growing stages of annual crops and also fallow ground can be simultaneously found from area to area, that cannot be correctly parameterized by a unique value only dependent on season.

Many different land surface parameterizations (LSP) schemes are found in the literature, assigning mean values of various biophysical properties to LULC categories, usually with seasonal dependence. Representativeness of these values can differ from site to site in different parts of the world, in function of the local characteristics of land covers included in the same category. Satellite remote sensing can be a practical method to overcome some of the above mentioned problems. There are many examples in the literature where inclusion of satellite derived products (both updated land cover maps and maps of some surface parameters) has been shown to be a valid help in improving simulations in meteorological and hydrological models (Pineda et al., 2004; Cheng et al., 2008).

To be routinely used in atmospheric modelling applications, operational methodologies of remote sensing data processing and suitable interfaces to feed models with that data are needed. With the aim of contributing to address these requirements, we used ASTER (Advanced Spaceborne Thermal Emission and reflectance Radiometer) data (NASA, 2008) to feed the atmospheric dispersion package Aria Industry (Arianet, 2001). In particular, the satellite image was used to update/integrate the CORINE Land Cover map and to directly calculate one of the needed parameters, namely the albedo.

2. DISPERSION MODELLING

The package Aria Industry is composed by three main models: the dispersion model SPRAY, the diagnostic meteorological model MINERVE and the turbulence model SURFPRO. SPRAY (Tinarelli et al., 1998) is a 3D lagrangian stochastic particle dispersion model able to simulate air pollution dispersion in non homogenous, non stationary conditions and over complex topography. The mean fluid velocity is calculated using the mass-consistent code MINERVE (Geai, 1987) that generates 3D fields of wind and temperature. SURFPRO generates the 2D atmospheric turbulence scale parameters fields from the wind and temperature field generated by MINERVE and from real meteorology data (cloud cover, pressure, relative humidity, solar radiation, precipitation). The scaling variables calculation, on the basis of the Monin-Obukhov similarity theory and surface energy budget evaluation (Van Ulden and Holtslag, 1985), starts from two dimensional arrays of surface parameters (roughness length, albedo, Bowen ratio, etc.) and ground meteorological parameters given as input. On the basis of the computed scaling variables, SPRAY calculates the 3D fluctuation of wind components according to parameterization codes described by Hanna (1982). Land surface forcing of atmospheric circulation is calculated starting from a two dimensional array of land use data, where land use categories are coded by a numerical value. Surface parameters affecting atmospheric

turbulence (roughness length, albedo, Bowen ratio, soil heat flux, leaf area index, canopy height and internal resistance) are retrieved directly from the 2D land use array through correspondence tables (LSP scheme) and used, together with some ground-level meteorological quantities given as input, for calculation of turbulence scale parameters. The Aria Industry package furnishes two precompiled schemes: the Aggregate CORINE scheme and the USGS/BATS scheme. The first of them was used for the present work.

3. MODIFICATION OF THE AGGREGATE CORINE LULC SCHEME

The Aggregate CORINE scheme used by SPRAY is based on the CORINE Land Cover (CLC) legend (EEA, 2006). It consists of 21 LULC categories roughly corresponding to the Level 2 of that classification and groups together the 44 classes of the CORINE Level 3 (L3). Each class is assigned with a set of default values of surface parameters (function of season when needed), that can be changed by the user.

As a preliminary step, we slightly modified the Aggregate CORINE scheme and the assignment of some L3 classes to the Aggregate categories, in order to improve representativeness of surface parameters values. At the present stage of the work, however, the default SPRAY values were not changed. The mentioned modifications were done on the basis of: 1) the definition of the L3 classes provided by the office responsible for Italian CLC data (APAT - Land - Environment Protection Agency); 2) actual appearance of some L3 classes in Italy; 3) comparison with other classification schemes available in the literature, namely from BATS (NCAR, 1993), PC RAMMET (U.S. EPA, 1995), MM5 (UCAR), Wieringa, 1993, and Oke, 1987; the class definition and the roughness length values were taken into account as the basis for the comparison with that schemes.

As a result, in the Aggregate CORINE scheme two classes were disaggregated into four and two classes were fused into others; six L3 classes changed their belonging to an Aggregate class. As an example, the L3 class “Green Urban areas” was moved from the Aggregate class “Other artificial surfaces” (which by default, was assigned the same parameters values as “Urban areas”) to “Heterogeneous agricultural areas”. The new obtained legend was used to run SPRAY using the available CLC maps.

The legend of the Aggregate CORINE scheme was further modified for use with remote sensing data. In particular two classes (“Cultivated land” and “Pastures”) were disaggregated into classes representing different phenological conditions and absence of vegetation (fallow ground), because these characteristics (usually accounted for with dependence on season) are retrievable from images. To assign surface parameters to the new classes, we used the default values of the original class for the season when the considered condition is predominant (e.g. the new class “Cultivated land: fallow ground” was assigned with the default Fall values of “Cultivated land”). This version of the Aggregate scheme was used to run SPRAY using the CLC maps integrated by remote sensing information.

4. STUDIED AREA AND DATASET

The work was carried out on a test area of 30 km x 40 km (simulation domain) at Venice (Northern Italy) (Figure 1). It is an almost flat coastal site characterized by sea-breeze development and complex LULC pattern, including urban and industrial areas, cultivated land, sea, lagoon and marsh areas. The domain origin (South-West corner) is located at cartographic coordinates 264 000 m East and 5 017 140 m North (UTM33-WGS84) and is centred on the big industrial site of Porto Marghera. Simulation was carried out for the period 5 - 15 September 2007.

The simulation was performed using real meteorological data provided by the Ente Zona of Porto Marghera and the Istituto Cavanis (Venice). Four ground stations, three located at Porto Marghera and one in the city of Venice, provided ground wind and temperature data, and a SODAR-RASS station (at Porto Marghera) provided wind and temperature profiles. These data were given as input to MINERVE to calculate 3D wind and temperature fields. Hourly time series of pressure, relative humidity, total solar radiation and precipitation from one of the ground stations were used to setup SURFPRO. The needed mean value of water temperature was obtained from the Veneto Sea Report (ARPA Veneto).

Surface topography was provided by the Digital Elevation Model from the Shuttle Radar Topography Mission (U.S. Geological Survey).

Land cover was extracted from the CLC2000 L3 data set (EEA, 2006).

The ASTER image used was acquired on 05 September 2007 at 10:07 GMT. ASTER acquires images in 14 spectral bands from visible to thermal infrared, with a spatial resolution from 15 m (visible-near infrared) to 90 m (thermal infrared). In this work the 3 bands in the Visible-Near Infrared, with a spatial resolution of 15 m and the 6 bands in the Short Wave Infrared, with a spatial resolution of 30 m, have been used. ASTER data were preliminary converted to ground reflectance, corrected for atmospheric effects and georeferenced.

5. LAND USE AND ALBEDO FROM ASTER IMAGE

The ASTER image was classified to generate an updated land cover map. A simple, standard approach is needed in order to make remote sensing a routine input to models. To this aim, an operational procedure for classification was

defined. This procedure includes a legend of cover types to be separated in the image. The legend contains covers easily separable by remote sensing and differing each other by bio-physical properties important for consequences on surface-atmosphere interactions. Differences in albedo were not accounted for in this legend, since this parameter was directly retrieved from the image. A standard procedure was then set to perform classification. It includes: 1) Separation of water using a threshold value on ASTER channel 3 (Near InfraRed); 2) Separation of vegetated and non vegetated cover types using a threshold value on a NDVI image (Normalized Difference Vegetation Index); 3) Masking of the image to produce a "vegetation" image and a "non vegetation" image; 3) Pre-processing of the "non vegetation" image for a better separation of non-vegetated covers (often separation among urban, industrial and bare soil is difficult due to similar spectral response), consisting in a Principal Component Analysis aimed to enhance subtle spectral differences; 4) Separated classification of "vegetation" and "non vegetation" images using the maximum likelihood algorithm, with training areas chosen with the help of high resolution Google Earth data. 5) Combination of the classifications into a single image.

Using this procedure, a land cover map of the studied area was produced. This map was used to update/increase the information content of the Aggregate CORINE Land Cover map obtained from the CLC2000 dataset.

In order to import the additional information from remote sensing, a set of rules was defined that control the way the remote sensing classification modifies the Aggregate CORINE Land Cover classes. The rules were chosen with the goal of maximizing the input of information where this input causes significant changes in the surface parameters, while minimizing the influence of possible errors in the remote sensing classification. For each Aggregate CORINE Land Cover class, the remote sensing classes that are allowed to change that class, and the corresponding destination class for each of them were set. For example, the remote sensing class "Industrial" changes all the Aggregate classes of vegetation into the Aggregate class "Industrial"; the remote sensing class "Fallow ground" changes the Aggregate class "Cultivated Land" into the newly added Aggregate class "Fallow ground", but the same class does not modify the Aggregate class "Industrial", since these two classes can be confused by remote sensing, and the possibility of an error is great, while the possible presence of areas of bare ground at an industrial site is normal and accounted for in the mean values of the parameters assigned to that class. On the contrary, the remote sensing class "Water" can change almost all the original Aggregate CORINE classes, because it leads strong differences in the values of surface parameters and is well separated by remote sensing (low possibility of errors).

Changes induced by remote sensing information on CLC2000 data were analysed building a matrix of the changes for each aggregate class. The Aggregate class "Cultivated land" is the most extended (46.6% of the studied area) and also that affected by deeper changes. As already quoted, this class was disaggregated into classes representing different phenological conditions using remotely sensed information. 47% of pixels in that class were reassigned to the class "Fallow ground-Stubbles". This fact has consequences on the values of the surface parameters used by the model: in fact Summer conditions are selected using CLC2000 data, since the period of simulation is late summer. Fall values are instead assigned to the class "Fallow ground-Stubbles". For example, roughness length changes from 0.2 to 0.05.

Surface albedo (α) has been computed for each pixel of the ASTER image using the relation of Liang S. (2000):

$$\alpha = 0.484 \cdot \rho_1 + 0.335 \cdot \rho_3 - 0.324 \cdot \rho_5 + 0.551 \cdot \rho_6 + 0.305 \cdot \rho_8 - 0.367 \cdot \rho_9 - 0.0015 \qquad (1)$$

where ρ_i is surface reflectance computed in the ASTER band *i*. Albedo was computed with a ground resolution of 30 m and then averaged for each cell of the dispersion simulation grid.

6. RUNS OF THE MODEL AND RESULTS

The aims of this part of the work are: 1) to evaluate the differences between dispersion modelling results obtained using the land use data set extracted only by CLC and those obtained using CLC integrated with remote sensing classification; 2) to evaluate the differences between dispersion modelling results obtained using tabulated values of surface albedo and those obtained using albedo retrieved from remote sensing. For this purpose three runs of the dispersion model have been done: R0) the land use data set is extracted only from CLC and albedo is estimated from the Aggregate CORINE Scheme. This configuration is assumed as the reference. R1) the land use data set is extracted from CLC and from remote sensing land use classification, albedo is the same as R0. R2) the land use is the same as R0 but albedo is evaluated from remote sensing. All the other parameters are the same for the three runs. The model outputs used to make quantitative comparisons are: roughness length (z_0), friction velocity (u^*), convective scale velocity (w^*), mixing height (h), Monin-Obukhov length (L) and number of particles (n).

The computational 3D grid defined for the studied area is made of 121, 161 and 30 points in the East, North and vertical directions respectively. The horizontal grid step is 250 m. The vertical step is variable: the first step is about 10 m and the top of the vertical domain is 1500 m. Time step is 1 h, for a total of 240 steps. Two hypothetic emission sources (chimneys) have been placed on the domain (see Fig. 1). These chimneys have the same geometrical and physical characteristics: they have a height of 100 m and a diameter of 4 m, the temperature of flue gases is 140 °C and efflux velocity of the gases is 10 ms^{-1}. Each source emits about 3240 particles h^{-1}, thus, for the 10 days period more than 1.5 million of particles are considered.

Table 1 summarises the comparison of output variables, excluding n, obtained from the R0 and R1 runs. Since the model uses different parameterizations for Land and for Water, and for day time and night time, the statistics are computed separately for each combination Land-Water and Day-Night. For each combination and for each variable the following statistics are reported: the mean value and the standard deviation obtained from runs R0 and R1; the Root Mean Square Difference (RMSD) between R1 and R0 values. The first consideration that can be carried out from these results is that in all the cases the two runs produced very similar mean and standard deviation values and, at the same time, significant values of RMSDs. This means that changes introduced by remote sensing land use classification are significant when considering the results at a spatial scale close to the grid spatial step, but their importance lowers when considering mean values at coarser scale. Moreover, these changes are more important over water than over land, and are more important during daytime than during nighttime.

Table 1. Comparison of results from model runs R0 and R1 (see text).

Variable (units)	Run	Land, Day		Land, Night		Water, Day		Water, Night	
		Mean, σ	RMSD	Mean, σ	RMSD	Mean, σ	RMSD	Mean, σ	RMSD
z_0 (cm)	R0	32.8, 30.8	17.3	32.8, 30.8	17.3	0.5, 2.3	6.5	0.5, 2.3	6.5
	R1	31.5, 34.4		31.5, 34.4		0.6, 6.0		0.6, 6.0	
u^* (ms^{-1})	R0	0.50, 0.21	0.10	0.25, 0.16	0.07	0.43, 0.27	0.19	0.24, 0.14	0.13
	R1	0.49, 0.21		0.25, 0.17		0.49, 0.25		0.29, 0.18	
w^* (ms^{-1})	R0	1.07, 0.63	0.12	0.03, 0.11	0.01	0.86, 0.39	0.34	0.72, 0.38	0.42
	R1	1.11, 0.65		0.03, 0.11		0.99, 0.36		0.89, 0.39	
L (m)	R0	-206, 357	125	45, 173	73	-278, 342	267	-30, 111	132
	R1	-190, 343		46, 177		-304, 321		-48, 138	
h (m)	R0	1163, 681	111	162, 130	50	676, 398	256	346,208	180
	R1	1202, 713		163, 136		772, 370		435, 244	

The comparison of particles number, for R0 and R1 runs, was made by considering the number of particles that transitated through a given surface cell. Surface cells are defined as ground based and with top at 20 m. This number ranges from 0 to 16. Also in this case, mean values and standard deviations obtained from the two runs can be considered the same: mean = 1.2, σ = 1.8. But when considering the number of surface cells that show n greater than a given threshold (n_t), some significant differences can be evidenced. Table 2 shows this comparison for different values of n_t. These results show that run R0 produces more cells with high particles number than run R1.

Table 2. Number of particles obtained from model runs R0 and R1 (see text).

Run	$n_t = 5$	$n_t = 6$	$n_t = 7$	$n_t = 8$	$n_t = 9$	$n_t = 10$
R0	$n = 1202$	$n = 710$	$n = 402$	$n = 213$	$n = 123$	$n = 74$
R1	$n = 1166$	$n = 659$	$n = 349$	$n = 185$	$n = 97$	$n = 55$
100 $(n_{R1}-n_{R0})/n_{R0}$	-3%	-6%	-13%	-13%	-21%	-26%

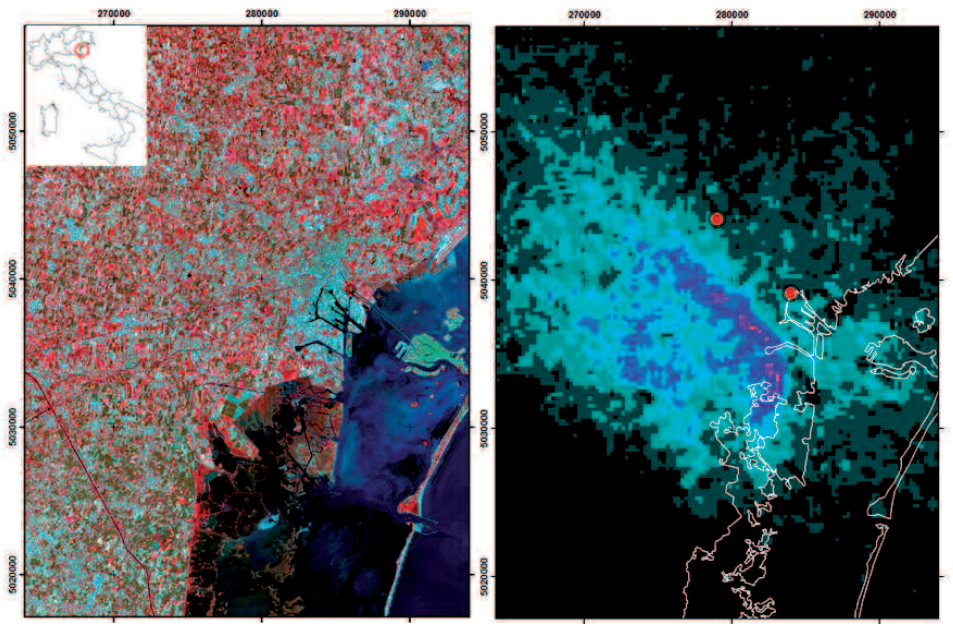

Figure 1. Left: ASTER image (false colour composition) of the studied domain; Right: total number of particles transitated through each cell. Red circles indicate location of emitting sources.

The first steps of the second test consisted in: calculating the albedo for each pixel of the ASTER image according to equation (1); calculating the average albedo values on each grid cell (250 m); extracting mean values and standard deviations of albedo for each land use class; comparing the obtained values with those tabulated in the Aggregate CORINE Scheme. Figure 2 shows the results of this comparison. Albedo values retrieved from remote sensing image are very close to the tabulated values for all the land use classes. The only exception is "Beach, dunes and sand plains" (num. 15) that covers less than 1% of the studied area. As a consequence of this preliminary result, the comparison between R0 and R2 values is not shown, since there are not significant differences."Water bodies" class has not been considered since, for this kind of surface, albedo is strongly dependent on sun elevation (tabulated value represents a daily mean, while ASTER furnishes an instantaneous value).

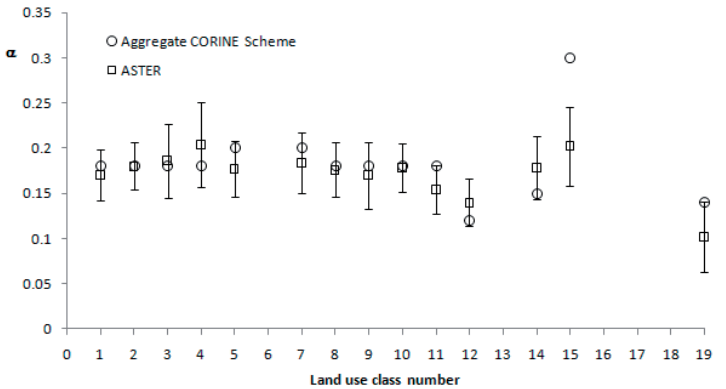

Figure 2. Albedo values for LULC classes tabulated in the Aggregate Corine Scheme and retrieved from ASTER image.

7. CONCLUSIONS

In this work it has been tested the importance of using surface information retrieved from ASTER satellite sensor for atmospheric dispersion modelled by the Aria Industry Package. In particular, two tests have been made to evaluate the differences on several turbulence variables produced by: 1) the integration of CORINE land use data base with land use information retrieved from ASTER image; 2) the use of surface albedo retrieved from ASTER image in place of that tabulated in the internal data base of the dispersion model. The first test shown that mean variable values and their standard deviations computed over the whole domain change vary little, but local (computing grid step scale) differences are important.

The second test shown that albedo retrieved from ASTER image is very close to the values reported in the model internal tables; this means that remote sensing images represent an alternative way of evaluating this important surface parameter.

REFERENCES

ARIANET, 2001: SPRAY 3.0 General Description and User's Guide.

Cheng, F.Y., S. Kim, and D.W. Byun, 2008: Application of high resolution land use and land cover data for atmospheric modeling in the Houston-Galveston metropolitan area: part II Air quality simulation results. *Atm. Environment*, **42**, 4853-4869.

EEA, 2006: European Topic Centre on Terrestrial Environment, URL:http://terrestrial.eionet.eu.int/ CLC2000.

Geai, P., 1987: Methode d'interpolation et de reconstitution tridimensionelle d'un champ de vent: Le code d'analyse objective MINERVE, Rep. ARD-AID: E34-E11, EDF, Chatou, France.

Hanna, R.S., A.G. Briggs, and P.R. Hosker, 1982: Handbook on atmospheric diffusion. Tech. Information Center, U.S.A.

Liang, S., 2000: Narrowband to broadband conversions of land surface albedo. I Algorithms. *Rem. Sen. of Environment*, **76**, 213-238.

NCAR, 1993: Biosphere-atmosphere transfer scheme (BATS) Version 1e as coupled to the NCAR community climate model. NCAR/TN-387+STR, Boulder, Colorado.

Oke, T.R., 1987: Boundary layer climates. 2nd Ed., Methuen, New York.

Pineda, N., O. Jorba, J. Jorge and J.M. Baldasano, 2004: Using NOAA AVHRR and SPOT VGT data to estimate surface parameters: application to a mesoscale meteorological model. *Int. J. Remote Sensing*, **25**, 129-143.

Tinarelli, G., D. Anfossi, M. Bider, E. Ferrero and S. Trini Castelli, 1998: A new high performance version of the Lagrangian particle dispersion model SPRAY, some case studies. *Proc. of the 23rd CCMS-NATO Meeting* (Varna, Bulgaria, September-October 1998) Kluwer Academic Publishers, 499–507.

UCAR, MM5 Community model, URL: http//www.mmm.ucar.edu/mm5/mm5-home.html.

U.S. E.P.A., 1995: PC RAMMET User's manual. Research triangle Park, N.C.

Van Ulden, A. P. and A. A. M. Holtslag, 1985: Estimation of atmospheric boundary layer parameters for diffusion application. *J. Clim. Appl. Meteor.*, **24**, 1196–1207.

Wieringa J, 1993: Representative roughness parameters for homogeneous terrain, *Boundary Layer Met.*, **63**, 323-363.